

## Article

# In Silico Screening of Bioactive Compounds of Representative Seaweeds to Inhibit SARS-CoV-2 ACE2-Bound Omicron B.1.1.529 Spike Protein Trimer

Muruganantham Bharathi <sup>1</sup>, Bhagavathi Sundaram Sivamaruthi <sup>1,2</sup>, Periyana Kesika <sup>2,\*</sup>,  
Subramanian Thangaleela <sup>1</sup> and Chaiyavat Chaiyasut <sup>1,\*</sup>

<sup>1</sup> Innovation Center for Holistic Health, Nutraceuticals, and Cosmeceuticals, Faculty of Pharmacy, Chiang Mai University, Chiang Mai 50200, Thailand; bharathi.m03@gmail.com (M.B.); sivamaruthi.b@cmu.ac.th (B.S.S.); drthangaleela@gmail.com (S.T.)

<sup>2</sup> Office of Research Administration, Chiang Mai University, Chiang Mai 50200, Thailand

\* Correspondence: kesika.p@cmu.ac.th (P.K.); chaiyavat@gmail.com (C.C.); Tel.: +66-53-944-340 (C.C.)

**Abstract:** Omicron is an emerging SARS-CoV-2 variant, evolved from the Indian delta variant B.1.617.2, which is currently infecting worldwide. The spike glycoprotein, an important molecule in the pathogenesis and transmissions of SARS-CoV-2 variants, especially omicron B.1.1.529, shows 37 mutations distributed over the trimeric protein domains. Notably, fifteen of these mutations reside in the receptor-binding domain of the spike glycoprotein, which may alter transmissibility and infectivity. Additionally, the omicron spike evades neutralization more efficiently than the delta spike. Most of the therapeutic antibodies are ineffective against the omicron variant, and double immunization with BioNTech-Pfizer (BNT162b2) might not adequately protect against severe disease induced by omicron B.1.1.529. So far, no efficient antiviral drugs are available against omicron. The present study identified the promising inhibitors from seaweed's bioactive compounds to inhibit the omicron variant B.1.1.529. We have also compared the seaweed's compounds with the standard drugs ceftriaxone and cefuroxime, which were suggested as beneficial antiviral drugs in COVID-19 treatment. Our molecular docking analysis revealed that caffeic acid hexoside (−6.4 kcal/mol; RMSD = 2.382 Å) and phloretin (−6.3 kcal/mol; RMSD = 0.061 Å) from *Sargassum wightii* (*S. wightii*) showed the inhibitory effect against the crucial residues ASN417, SER496, TYR501, and HIS505, which are supported for the inviolable omicron and angiotensin-converting enzyme II (ACE2) receptor interaction. Cholestan-3-ol, 2-methylene-, (3beta, 5 alpha) (CMBA) (−6.0 kcal/mol; RMSD = 3.074 Å) from *Corallina officinalis* (*C. officinalis*) manifested the strong inhibitory effect against the omicron RBD mutated residues LEU452 and ALA484, was magnificently observed as the essential residues in Indian delta variant B.1.617.2 previously. The standard drugs (ceftriaxone and cefuroxime) showed no or less inhibitory effect against RBD of omicron B.1.1.529. The present study also emphasized the pharmacological properties of the considered chemical compounds. The results could be used to develop potent seaweed-based antiviral drugs and/or dietary supplements to treat omicron B.1.1529-infected patients.

**Keywords:** SARS-CoV-2; omicron B.1.1529; seaweeds; *Sargassum wightii*; *Corallina officinalis*



**Citation:** Bharathi, M.; Sivamaruthi, B.S.; Kesika, P.; Thangaleela, S.; Chaiyasut, C. In Silico Screening of Bioactive Compounds of Representative Seaweeds to Inhibit SARS-CoV-2 ACE2-Bound Omicron B.1.1.529 Spike Protein Trimer. *Mar. Drugs* **2022**, *20*, 148. <https://doi.org/10.3390/md20020148>

Academic Editor: Diana Cláudia Pinto

Received: 2 February 2022

Accepted: 14 February 2022

Published: 17 February 2022

**Publisher's Note:** MDPI stays neutral with regard to jurisdictional claims in published maps and institutional affiliations.



**Copyright:** © 2022 by the authors. Licensee MDPI, Basel, Switzerland. This article is an open access article distributed under the terms and conditions of the Creative Commons Attribution (CC BY) license (<https://creativecommons.org/licenses/by/4.0/>).

## 1. Introduction

Omicron B.1.1.529 variant was first reported to World Health Organization (WHO) from South Africa on 24 November 2021 [1]. In South Africa, the epidemiological circumstance has been characterized by three distinct peaks in confirmed incidents, the most recent predominated by the Indian Delta variant B.1.617.2 [2]. On 26 November 2021, the World Health Organization's Technical Advisory Group on Virus Evolution (TAG-VE) proposed that variant B.1.1.529, referred to as omicron, be designated as a variant of concerns (VOCs) [1]. Infections have increased dramatically in recent weeks, coinciding with

the global detection of the omicron B.1.1.529 variant. Globally, the number of countries registering SARS-CoV-2 omicron B.1.1.529 infections keeps climbing, with 117 countries reporting 354 million confirmed cases as of 15 January 2022 [3]. Due to the widely altered omicron variant, many nations have imposed travel restrictions or border closures, and extensive research is desperately required for medical examinations and border closure advantages [4].

In the receptor-binding domain (RBD), the crucial mutations G446S, N501Y, G496S, Y505H, Q493R, E484A, T478K, S477N, K417N, G339D, S371L, S373P, S375F, N440K, and Q498R occur in the RBD of omicron B.1.1.529 variant [5–7]. The mutated residues Q493R, G496S, and Q498R, in particular, strengthen RBD adherence to the angiotensin-converting enzyme 2 (ACE2) receptor [5,8]. Additionally, the N501Y mutation localizes at RBD, which might help attain higher binding to host cells and result in elevated transmission and infectiousness [9]. Similarly, the mutation in E484K, K417N/K417T, and N501Y plays a vital role in the RBD and the ACE2 receptor binding of the beta (B.1.351) and gamma (P.1) variants. Therefore, B.1.351 and P.1 were designated as VOCs in early 2021, an outbreak in South Africa and Brazil [10–12].

Omicron B.1.1.529 has many nonsynonymous mutations in the RBD, including in L452R, and E484K, which significantly neutralize the activity of multiple monoclonal antibodies (mAbs) [13,14]. Omicron may be more contagious than any other identified variant, and more than twice as infectious as the delta variant B.1.617.2, possibly due to the mutations in N440K, T478K, and N501Y [15,16]. Moreover, omicron has the potential to disrupt the binding of most 185 mAbs, indicating more vaccine-breakthrough potential than delta or any other identified variations [17].

The world demands innovative antiviral medications that are efficient at halting viral propagation without exerting further selection pressure on resistant variants [18]. Aside from upgrading vaccinations against omicron or future variants, we must accelerate the discovery of novel antivirals [19].

Seaweeds are important resources from coastal ecosystems, contributing considerably to the trophic structure [20,21]. Furthermore, seaweeds provide several bioactive compounds with antiviral, anticancer, and anticoagulant activity and help manage conditions like obesity and diabetes [22–24].

One of the main processes involved in viral proliferation and subsequent diseases is the overproduction of reactive oxygen species (ROS) and the depletion of antioxidant systems [25,26]. The sulfated polysaccharides derived from *Corallina officinalis* (*C. officinalis*) would be used as a natural antioxidant in the food manufacturing industry [27,28]. *Caulerpa racemosa* (*C. racemosa*) could be a rich source of novel antioxidant and anti-inflammatory agents. However, the bioactive chemicals must be separated and purified to study the exact mechanism of action [29,30]. Furthermore, increasing soluble Fas and B-cell CLL/lymphoma-2 (Bcl2) levels in COVID-19 patients raises the fatality rate in COVID-19 individuals [31]. However, *Colpomenia sinuosa* (*C. sinuosa*)-treated HCT-116 cells have downregulated anti-apoptotic Bcl 2, which leads to caspases activation [32].

*Gracilaria edulis* (*G. edulis*) and *Gracilaria corticata* (*G. corticata*) possess greater levels of essential n-3 polyunsaturated fatty acid (PUFA), which inhibits the establishment of atherosclerotic plaque, blood coagulation, and blood pressure, as well as boost immunological function [33,34].

*Padina boergesenii* (*P. boergesenii*) might contain bioactive chemicals with substantial antibiotic action and play an important role in drug discovery [35].

*Sargassum wightii* (*S. wightii*) is a brown seaweed containing several bioactive compounds such as fucoidan and fucoxanthin, and substantial quantities of polyphenols and flavonoids play a vital role in anticoagulant, antithrombotic, immunomodulation, anti-cancer, and antiviral activity [36,37].

The phytochemicals of *C. officinalis*, *C. racemosa*, *C. sinuosa*, *G. edulis*, *G. corticata*, *P. boergesenii*, *S. wightii*, and *U. fasciata* were used in this study to find potent inhibitors of SARS-CoV-2 ACE2-bound omicron B.1.1.529 spike protein trimer. We conducted the molec-

ular docking study using Autodock Vina [38] with Pyrx v0.8 [39], Pymol v2.5 [40], Ligplot+ v2.2.4 [41], and Discovery Studio Visualizer v21.1.0.20298. We also assessed the drug-likeness, adsorption, digestion, metabolism, excretion, toxicity (ADMET), toxicity class, and a lethal dosage study for the finalized chemical compounds using the Molinspiration server [42], ADMETlab 2.0 [43], and ProTox-II [44].

## 2. Materials and Methods

### 2.1. Chemical Compounds from Seaweeds

A sum of 96 chemical compounds from seven seaweeds (*C. officinalis*, *C. racemosa*, *C. sinuosa*, *G. edulis*, *G. corticata*, *P. boergeresii*, *S. wightii*, and *U. fasciata*) was subjected to evaluate the interaction with the RBD of S-protein of omicron variant B.1.1.529.

### 2.2. Target Preparation and Ligand Library

Cryo-EM structure of the ACE2 binding, spike protein of SARS-CoV-2 omicron spike PDB: 7T9J [5], was retrieved from protein data bank and exported in Protein Data Bank (PDB) format [45]. The major chemical compounds of the selected seaweeds were retrieved in Spatial Data File (SDF) format and 2D structures from the PubChem database [46]. For the acquired 2D structures, the 3D structure was delineated and optimized with the force field relying on Chemistry at Harvard Macromolecular Mechanics (CHARMM) approximation using ACD/Chemsketch vC05E41 (Advanced Chemistry Development, Inc., Toronto, Canada) and saved as SDF formats. The 3D structure of all chemical compounds was then transformed to the PDB format for the further docking process using the OPEN BABEL program [47].

### 2.3. Molecular Docking

After preparing the chemical compounds as ligands, and RBD from 7T9J as a target, we implemented the Autodock Vina for the molecular docking process using PyRx software [38,39]. It examines the docking propensity of the ligands and the interfaces between the ligands and the RBD residues. The prepared targets and ligands were saved in PDBQT format. We used the PyRx virtual screening tool for the docking analysis to identify the crucial ligands, which inhibit the ACE2 binding residues. The size was assigned to the grid box properties as size\_x = 67.33 Å, y = 74.87 Å, and size\_z = 106.22 Å, and the ligands were docked with the RBD. The ligands were chosen based on their binding affinity ( $\leq 6.0$  kcal/mol.) by importing the docked data into PyMol [40], Lig-Plot+ [41] and Discovery Studio Visualizer v19.1.0.1828 (Dassault Systèmes BIOVIA, Rue Marcel Dassault, Vélizy-Villacoublay-78140, France, [www.accelerys.com](http://www.accelerys.com) (accessed on 6 January 2022)), and the substantial association for both the ligands and the receptors' binding site was obtained in 2D and 3D format. Auto dock vina scoring function was employed.

$$C = \sum_{i < j} f_{titj}(r_{ij})$$

where  $C$  is the sum of intermolecular and intramolecular distances;  $\Sigma$  is atoms separated by three consecutive covalent bonds;  $f_{titj}$  is the symmetric set of interaction functions;  $r_{ij}$  is interatomic distance.

### 2.4. Evaluation of Ligands Drug-Likeness and Toxicity

Using the Molinspiration server ([www.molinspiration.com/cgi-bin/properties](http://www.molinspiration.com/cgi-bin/properties) (accessed on 15 January 2022)), the finished ligands were tested for drugability, physicochemical characteristics, toxicity, toxicity classes, and fatal dosage. The drugability characteristics were evaluated using molinspiration lipophilicity (Mi log P), molar weights (MW), total polar surface area (TPSA), number of rotatable atoms (natoms), hydrogen bond acceptor (HBA), and hydrogen bond donor (HBD). Lipinski's rule of the drug-like compounds was determined. In addition, the PubChem Database [46] was used to download the simplified molecular-input line-entry system (SMILES) to compute ADMET characteristics with toxic-

ity class. The ADMET properties were calculated using ADMETlab 2.0 [43] and ProTox-II with default parameters [44].

### 3. Results

The cryo-EM structure of the ACE2 binding RBD of omicron B.1.1.529 spike protein (PDB: 7T9J) with the RMSD of 2.79 Å [5] is depicted with its mutation in Figure 1.

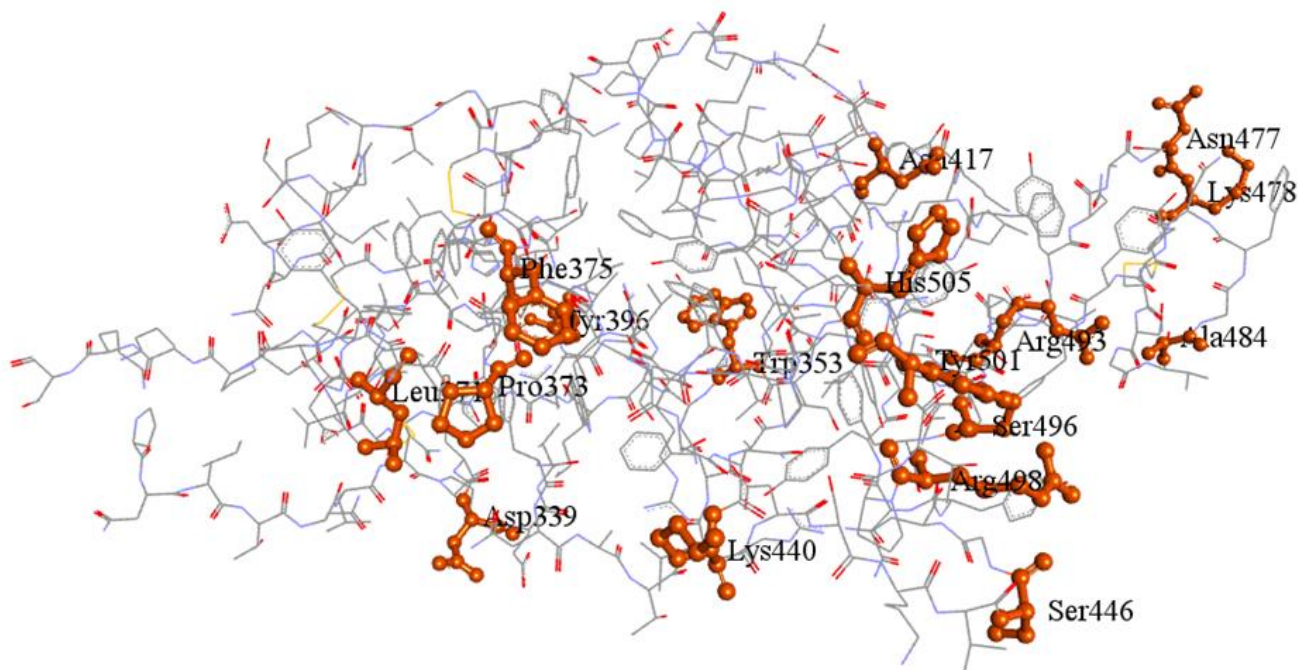


**Figure 1.** The cryo-EM structure of the RBD of spike protein of SARS-CoV-2 omicron B.1.1.529 (PDB: 7T9J). The critically mutated regions are highlighted in orange.

The effects of chemical compounds from *C. officinalis*, *C. racemosa*, *C. sinuosa*, *G. edulis*, *G. corticata*, *P. boergesenii*, *S. wightii*, and *U. fasciata* were analyzed to understand the binding efficiency against the omicron spike protein of RBD (Table S1; Supplementary File S1). The chemical properties, including molecular formula, molecular weight, and PubChem ID for the seaweed compounds, which showed significant activity against the RBD of omicron spike protein (binding affinity  $\leq -6.0$  kcal/mol) were listed (Table 1), and its Ligplot interactions were analyzed and represented (Figure S1; Supplementary File S1).

**Table 1.** The properties of screened phytocompounds with the binding energy of  $\leq -6.0$  kcal/mol against RBD domain of omicron B.1.1.529 spike protein.

| Seaweeds Name         | Compound Name   | Molecular Formula  | Mol. Weight (g/mol) | PubChem ID |
|-----------------------|---|--|---------------------|------------|
| Standard drug         | Ceftriaxone   | C <sub>18</sub> H <sub>18</sub> N <sub>8</sub> O <sub>7</sub> S <sub>3</sub> | 554.6               | 5479530    |
|                       | Cefuroxime  | C <sub>16</sub> H <sub>16</sub> N <sub>4</sub> O <sub>8</sub> S              | 424.4               | 5479529    |
| <i>C. officinalis</i> | 3',8,8'-Trimethoxy-3-piperidin-1-yl-2,2'-binaphthyl-1,1',4,4'-tetrone | C <sub>28</sub> H <sub>25</sub> NO <sub>7</sub>                              | 487.5               | 590815     |
|                       | Cholestan-3-ol, 2-methylene-, (3beta, 5 alpha)                        | C <sub>28</sub> H <sub>48</sub> O  | 400.7               | 22213932   |
| <i>C. racemosa</i>    | Glucobrassicin  | C <sub>16</sub> H <sub>20</sub> N <sub>2</sub> O <sub>9</sub> S <sub>2</sub> | 448.5               | 656506     |
|                       | Matairesinol  | C <sub>20</sub> H <sub>22</sub> O <sub>6</sub>                               | 358.4               | 119205     |
| <i>C. sativa</i> L    | Naringenin  | C <sub>15</sub> H <sub>12</sub> O <sub>5</sub>                               | 272.25              | 932        |
|                       | Syringaresinol  | C <sub>22</sub> H <sub>26</sub> O <sub>8</sub>                               | 418.4               | 100067     |

Table 1. Cont.

| Seaweeds Name         | Compound Name   | Molecular Formula  | Mol. Weight (g/mol) | PubChem ID |
|-----------------------|---|--|---------------------|------------|
| <i>G. corticate</i>   | Bicyclo[3.2.1]oct-3-en-2-one, 3,8-dihydroxy-7-(7-methoxy-1,3-benzodioxol-5-yl)-6-methyl-5-(2-propenyl)-, [1S-(6-endo,7-exo,8-syn)]- | C <sub>20</sub> H <sub>22</sub> O <sub>6</sub>                               | 358.39              | 101282028  |
|                       | Cholesta-8,24-dien-3-ol, 4-methyl-, (3.beta.,4.alpha.)-   | C <sub>28</sub> H <sub>46</sub> O  | 398.7               | 22212496   |
|                       | Glucobrassicin  | C <sub>16</sub> H <sub>20</sub> N <sub>2</sub> O <sub>9</sub> S <sub>2</sub> | 448.5               | 656506     |
| <i>P. boergesenii</i> | Glycitein   | C <sub>16</sub> H <sub>12</sub> O <sub>5</sub>                               | 284.26              | 5317750    |
|                       | Matairesinol  | C <sub>20</sub> H <sub>22</sub> O <sub>6</sub>                               | 358.4               | 119205     |
|                       | Naringenin  | C <sub>15</sub> H <sub>12</sub> O <sub>5</sub>                               | 272.25              | 932        |
|                       | Pyrano [4,3-b] benzopyran-1,9-dione, 5amethoxy-9amethyl-3-(1-propenyl)perhydro  | C <sub>17</sub> H <sub>24</sub> O <sub>5</sub>                               | 308.4               | 5364482    |
|                       | Syringaresinol  | C <sub>22</sub> H <sub>26</sub> O <sub>8</sub>                               | 418.4               | 100067     |
| <i>S. wightii</i>     | 5-p-coumaroylquinic acid  | C <sub>16</sub> H <sub>18</sub> O <sub>8</sub>                               | 338.31              | 6441280    |
|                       | Caffeic acid hexoside   | C <sub>15</sub> H <sub>18</sub> O <sub>9</sub>                               | 342.3               | 6124135    |
|                       | Phloretin   | C <sub>15</sub> H <sub>14</sub> O <sub>5</sub>                               | 274.27              | 4788       |
|                       | Quercetin-3-O-arabinoglucoside  | C <sub>26</sub> H <sub>28</sub> O <sub>16</sub>                              | 596.5               | 5484066    |

The phytochemicals interacting with the RBD residues of omicron spike protein, binding affinity, RMSD, and its interacting residues are listed in Table 2. The chemical compounds based on the crucial residue interactions such as PRO373, PHE375, TYR396, ASN417, LYS440, LEU452, ALA484, SER496, TYR501, and HIS505 and the binding affinity  $\leq -6.0$  kcal/mol were analyzed for the ADEMT properties such as drug-likeness, lethal dose, and toxicity classes and are represented in Table 3.

**Table 2.** The binding affinity, RMSD, and interacting residues of the screened phytochemicals against RBD domain of omicron B.1.1.529. spike protein with the resolution of 2.79Å.

| Seaweeds              | Chemical Compound   | Binding Affinity | RMSD (Å) | H/C-H Bond Interaction                         | Interaction Distances              | Hydrophobic Interaction  | Alkyl Interaction                      | Pi-Sigma /Cation Stacked Interaction |
|-----------------------|---|------------------|----------|--|------------------------------------|--|--|--------------------------------------|
| Standard drug         | Ceftriaxone   | -7.1             | 43.189   | ARG403, ASN417, TYR453, SER494, SER496, TYR501 | 5.36, 4.21, 6.03, 3.24, 3.59, 6.23 | ASP405, GLU406, ARG408, GLN409, LEU455, ARG493                         | -                                      | ARG403, HIS505                       |
|                       | Cefuroxime  | -5.3             | 2.483    | THR376, GLY404*, ARG408, TYR508                | 4.52, 5.06, 4.71, 5.71             | PHE375, ASN437   | ARG408, VAL503                         | -                                    |
| <i>C. officinalis</i> | 3',8,8'-Trimethoxy-3-piperidin-1-yl-2,2'-binaphthyl-1,1',4,4'-tetrone | -6.9             | 1.897    | -  | -                                  | ARG355, TYR396, ASP428, PHE429, THR430, SER514, PHE515, LEU517, LEU518 | PRO426, PRO463                         | PHE464, GLU516                       |
|                       | Cholestan-3-ol, 2-methylene-, (3beta, 5 alpha)                        | -6.0             | 3.074    | SER494   | 4.22                               | GLY482, THR470   | LEU452, TYR449, ILE472, ALA484, PHE490 | PHE490                               |
| <i>C. racemosa</i>    | Glucobrassicin  | -6.8             | 1.521    | ARG457, ARG466, ASP467, ASP467*                | 4.45, 6.50, 3.18, 5.49             | ARG454, PHE456, SER459, GLU465, ILE468, SER469, TYR473, PRO491         | ARG457, LYS458                         | ARG457, ASP467, GLU471               |

Table 2. Cont.

| Seaweeds              | Chemical Compound   | Binding Affinity | RMSD (Å) | H/C-H Bond Interaction                           | Interaction Distances                        | Hydrophobic Interaction  | Alkyl Interaction                      | Pi-Sigma /Cation Stacked Interaction |
|-----------------------|---|------------------|----------|--|--|--|--|--------------------------------------|
| <i>G. corticata</i>   | Bicyclo[3.2.1]oct-3-en-2-one, 3,8-dihydroxy-1-methoxy-7-(7-methoxy-1,3-benzodioxol-5-yl)-6-methyl-5-Cholesta-8,24-dien-3-ol, 4-methyl-, (3.beta.,4.alpha.)- | -6.3             | 20.322   | THR430   | 4.16   | ARG355, ASP428, SER514, PHE515, GLU516, LEU517                         | TYR396, PRO426, PHE429, PRO463, PHE464 | -                                    |
|                       | Glucobrassicin  | -6.8             | 1.544    | -  | -  | TYR396, ASP428, THR430, GLU465, SER514, PHE515, GLU516                 | PRO426, LYS462, PRO463, PHE464         | -                                    |
|                       | Glycitein   | -6.1             | 11.668   | ARG454, LYS458, SER459, SER469, THR376, ASP405 * | 5.00, 4.44, 2.38, 3.25<br>4.71, 4.5          | PHE456, ARG457, TYR473, PRO491, GLY404, ARG408, VAL503, GLY504         | -                                      | ASP467, GLU471                       |
| <i>P. boergesenii</i> | Matairesinol  | -6.0             | 1.707    | ARG355, PHE464 *, SER514                         | 6.65, 4.98, 3.72                             | TYR396, ASP428, PHE429, THR430, PRO463, PHE515, GLU516, LEU517         | PRO426                                 | -                                    |
|                       | Naringenin  | -6.4             | 20.209   | ASN437, LYS440, LEU441                           | 4.09, 4.44, 4.14                             | ASN343, PHE374, PHE375, SER438, ASN439                                 | PRO373, LYS440                         | TRP436                               |
|                       | Pyrano [4,3-b] benzopyran-1,9-dione, 5a-methoxy-9a-methyl-3-(1-propenyl) perhydro   | -6.1             | 29.617   | SER496, TYR501                                   | 3.39, 5.24                                   | ARG403, TYR453, TYR495, GLY502   | HIS505                                 | TYR501, HIS505                       |
| <i>S. wightii</i>     | Syringaresinol  | -6.4             | 0.44     | ARG355, ASP427 *, PRO463 *, PHE515 *, GLU516     | 6.88, 4.19, 4.81, 7.35, 3.78                 | ASP428, THR430, SER514   | TYR396, PRO426, LYS462, PRO463         | PHE464                               |
|                       | 5-p-coumaroylquinic acid  | -6.0             | 4.96     | ARG403, ASN417, TYR453, SER496                   | 5.43, [2.96, 4.87], 5.62, 3.42               | GLN409, GLY416, ILE418, LEU455, SER494, TYR495, TYR501, HIS505         | -                                      | -                                    |
|                       | Caffeic acid hexoside   | -6.4             | 2.82     | ARG403, GLU406, ASN417, TYR453, SER496           | [5.38, 6.24], 3.95, 4.96, 5.76, [3.34, 3.36] | ASP405, ARG408, GLN409, ILE418, LEU455, TYR495, SER494, TYR501, HIS505 | -                                      | -                                    |
|                       | Phloretin   | -6.3             | 0.061    | TYR501, SER496, TYR453                           | 5.37, 1.49, 5.90                             | ARG403, TYR495, PHE497, THR500, GLY502                                 | -                                      | TYR501, HIS505                       |
|                       | Quercetin-3-O-arabinoglucoside  | -6.1             | 2.248    | ASN331, THR333, GLY526, PRO527 *, LYS528C        | 5.09, [3.47, 3.38], [3.93, 4.29], 4.60, 5.10 | PRO330, ILE332, CYS361, THR523   | VAL362, CYS525                         | ASN360                               |

Note: \* = Carbon-hydrogen bond.

**Table 3.** Drug-likeness and toxicity analysis for the selected compounds that inhibits the RBD of omicron B.1.1.529. spike protein.

| Seaweeds              | Chemical Compounds  | Drug-Likeness |        |        |     |       |             | Toxicity Analysis     |                        |                        |                     |                       |                       |              |    |
|-----------------------|---|---------------|--------|--------|-----|-------|-------------|-----------------------|------------------------|------------------------|---------------------|-----------------------|-----------------------|--------------|----|
|                       |   | Mi LogP       | TPSA   | natoms | nON | nOHNH | #Violations | Intestinal Absorption | Hepato Toxicity        | Carcinogenicity        | Immuno toxicity     | Muta Genicity         | Cyto toxicity         | LD50 (mg/kg) | TC |
| Standard Drug         | Cefuroxime  | −0.98         | 173.77 | 29     | 12  | 4     | 1           | 0.065                 | 0.66 <sup>(Mild)</sup> | 0.50 <sup>(Mod)</sup>  | 0.99 <sup>(−)</sup> | 0.76 <sup>(−)</sup>   | 0.54 <sup>(Mod)</sup> | 10,000       | VI |
| <i>C. officinalis</i> | 3',8,8'-Trimethoxy-3-piperidin-1-yl-2,2'-binaphthyl-1,1',4,4'-tetrone | 3.99          | 99.22  | 36     | 8   | 0     | 0           | 0.606                 | 0.83 <sup>(−)</sup>    | 0.55 <sup>(Mod)</sup>  | 0.70 <sup>(+)</sup> | 0.56 <sup>(Mod)</sup> | 0.58 <sup>(Mod)</sup> | 400          | IV |
|                       | Cholestan-3-ol, 2-methylene-, (3beta, 5alpha)                         | 8.11          | 20.23  | 29     | 1   | 1     | 1           | 0.922                 | 0.94 <sup>(−)</sup>    | 0.62 <sup>(Mild)</sup> | 0.98 <sup>(+)</sup> | 0.94 <sup>(−)</sup>   | 0.94 <sup>(−)</sup>   | 5000         | V  |
| <i>G. corticate</i>   | Cholesta-8,24-dien-3-ol, 4-methyl-, (3beta,4.alpha.)-                 | 7.96          | 20.23  | 29     | 1   | 1     | 1           | 0.931                 | 0.82 <sup>(−)</sup>    | 0.58 <sup>(Mod)</sup>  | 0.97 <sup>(+)</sup> | 0.94 <sup>(−)</sup>   | 0.96 <sup>(−)</sup>   | 2000         | IV |
| <i>P.boergesenii</i>  | Syringaresinol  | 2.62          | 95.86  | 30     | 8   | 2     | 0           | 0.599                 | 0.87 <sup>(−)</sup>    | 0.54 <sup>(Mod)</sup>  | 0.95 <sup>(+)</sup> | 0.84 <sup>(−)</sup>   | 0.99 <sup>(−)</sup>   | 1500         | IV |
| <i>S. wightii</i>     | Caffeic acid hexoside   | −0.77         | 156.91 | 24     | 9   | 6     | 1           | 0.221                 | 0.82 <sup>(−)</sup>    | 0.76 <sup>(−)</sup>    | 0.95 <sup>(+)</sup> | 0.78 <sup>(−)</sup>   | 0.87 <sup>(−)</sup>   | 5000         | V  |
|                       | Phloretin   | 2.66          | 97.98  | 20     | 5   | 4     | 0           | 0.427                 | 0.63 <sup>(Mod)</sup>  | 0.72 <sup>(mild)</sup> | 0.98 <sup>(−)</sup> | 0.88 <sup>(−)</sup>   | 0.82 <sup>(−)</sup>   | 500          | IV |

Note: Mod = Moderate; − = Negative effect; + = Positive effect.

The standard drug, cefuroxime, evidenced the hydrogen bonding interactions with THR376, ARG408, and TYR508, and interacted with ARG408, VAL503 through the pi-alkyl bond. It also interacted with the residue GLY404 using a carbon–hydrogen bond and was surrounded by hydrophobic residues such as PHE375 and ASN437 with the binding affinity of  $-5.3$  kcal/mol and RMSD of  $2.483$  Å. Furthermore, cefuroxime interacted with one crucial mutated residue of RBD, PHE375, with a lower binding affinity (Figure 2A–C). Additionally, cefuroxime toxicity classes were predicted as VI. The 3',8,8'-Trimethoxy-3-piperidin-1-yl-2,2'-binaphthyl-1,1',4,4'-tetrone (TPBT) from *C. officinalis* formed the pi-sigma and pi-cation interaction with PHE464 and GLU516, a pi-alkyl interaction with PRO426 and PRO463, and a hydrophobic interaction with ARG355, TYR396, ASP428, PHE429, THR430, SER514, PHE515, LEU517, and LEU518 residues with the binding affinity of  $-6.9$  kcal/mol and RMSD of  $1.897$  Å. Likewise, the toxicity class was predicted as IV due to its moderate carcinogenic, immunogenic, mutagenic, and cytotoxic effects (Figure 2D–F). Similarly, cholestan-3-ol, 2-methylene-, (3 beta, 5 alpha) interacted with SER494 and PHE490 through hydrogen and pi-sigma bond and also interacted with the residues LEU452, TYR449, ILE472, ALA484, and PHE490 through alkyl interaction, surrounded by the hydrophobic residues GLY482 and THR470 with the binding affinity of  $-6.0$  kcal/mol, and RMSD of  $3.074$  Å. The toxicity class was predicted as V because of its positive effect on immunogenicity (Figure 2G–I).

Syringaresinol from *P. boergeresii* interacted with ARG355, ASP427 \*, PRO463 \*, PHE515 \*, and GLU516 through the hydrogen and carbon–hydrogen bond with the binding affinity of  $-6.4$  kcal/mol and RMSD of  $0.44$  Å. It also extended its pi-sigma and pi-alkyl interaction with PHE464, TYR396, PRO426, LYS462, and PRO463. Additionally, syringaresinol was surrounded by hydrophobic residues such as ASP428, THR430, and SER514. The toxicity class was predicted as IV, described by moderate carcinogenicity and a positive immunotoxic effect (Figure 2J–L).

Caffeic acid hexoside from *S. wightii* interacted with ARG403, GLU406, ASN417, TYR453, and SER496 via hydrogen bond with the binding affinity of  $-6.4$  kcal/mol and RMSD of  $2.82$  Å. It was also surrounded by hydrophobic residues such as ASP405, ARG408, GLN409, ILE418, LEU455, TYR495, SER494, TYR501, and HIS505. The toxicity class was identified as V, which also showed a positive effect on immunotoxicity (Figure 2M–O). Phloretin had a hydrogen bond interaction with TYR501, SER496, and TYR453 with the binding affinity of  $-6.3$  kcal/mol and RMSD of  $0.061$  Å. It also exhibited the interaction with the residues TYR501 and HIS505 via pi-pi-stacked bond, surrounded by hydrophobic residues such as ARG403, TYR495 PHE497, THR500, and GLY502. The predicted toxicity class for phloretin was IV, which indicated moderate hepatotoxic and mild carcinogenic effects (Figure 2P–R).

The Ligplot interactions for cefuroxime, TPBT, cholestan-3-ol, 2-methylene-, (3 beta, 5 alpha), syringaresinol, caffeic acid hexoside, and phloretin with the RBD were interpreted and are depicted in Figure 3A–F. The standard drug, ceftriaxone, interacted with ARG403, ASN417, TYR453, SER494, SER496, and TYR501 by hydrogen bond and formed the pi-alkyl interactions with ARG403 and HIS505. It was surrounded by hydrophobic residues such as ASP405, GLU406, ARG408, GLN409, LEU455, and ARG49 with the binding affinity of  $-7.1$  kcal/mol, and RMSD of  $43.189$  Å (Table 2). However, according to the observed RMSD ( $43.189$  Å), ceftriaxone did not interact with the RBD of omicron B.1.1.529 spike protein.

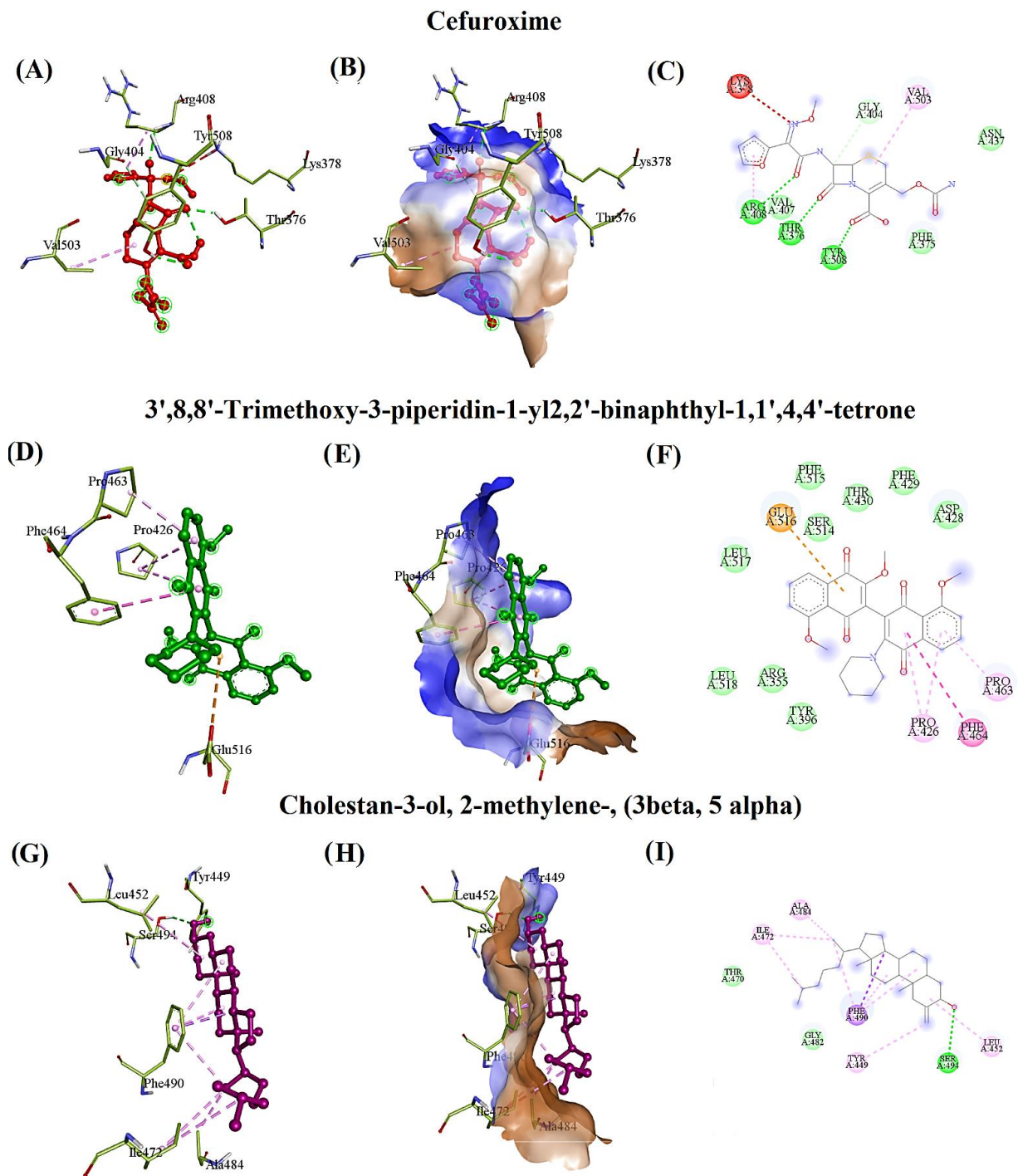
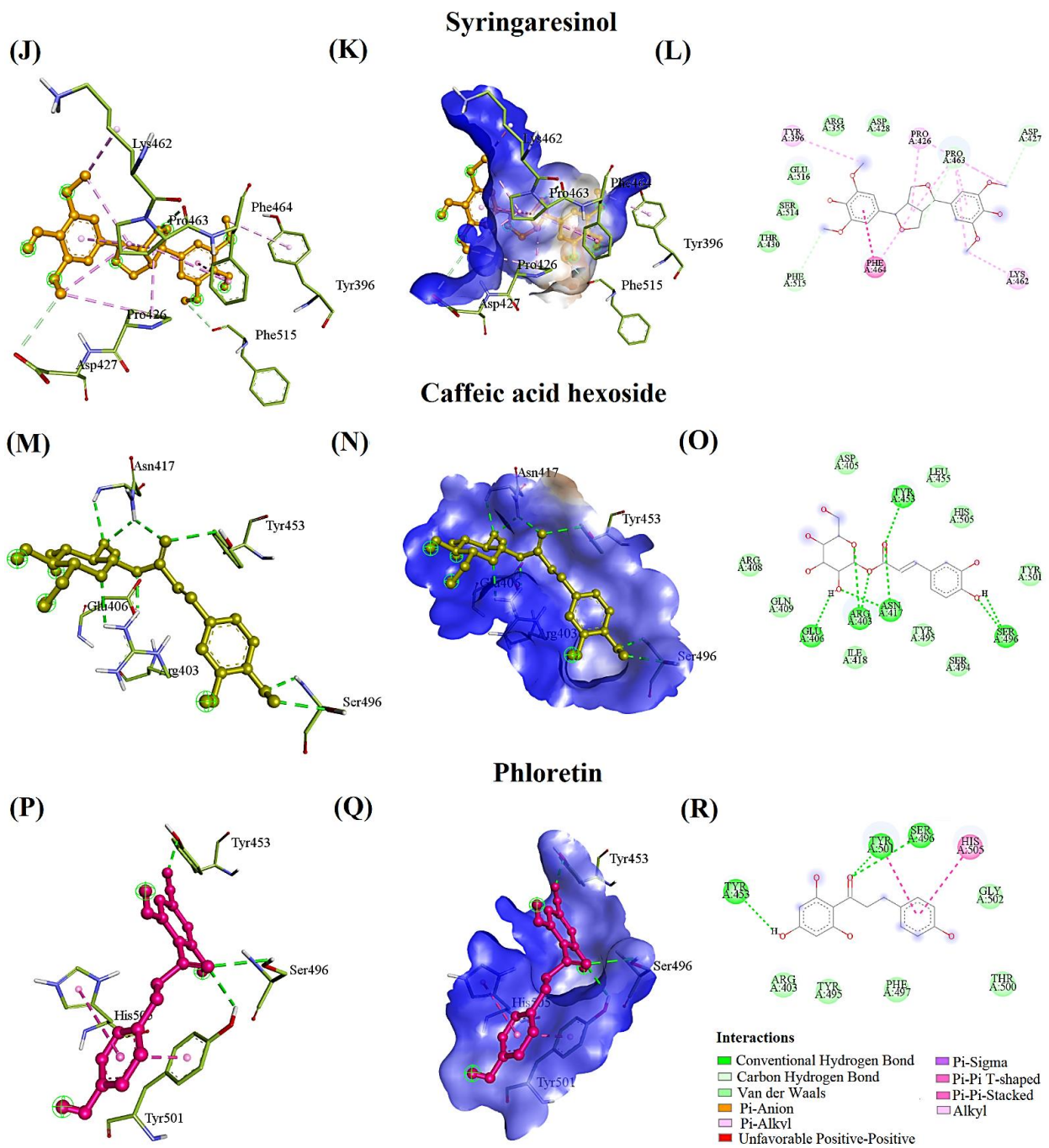
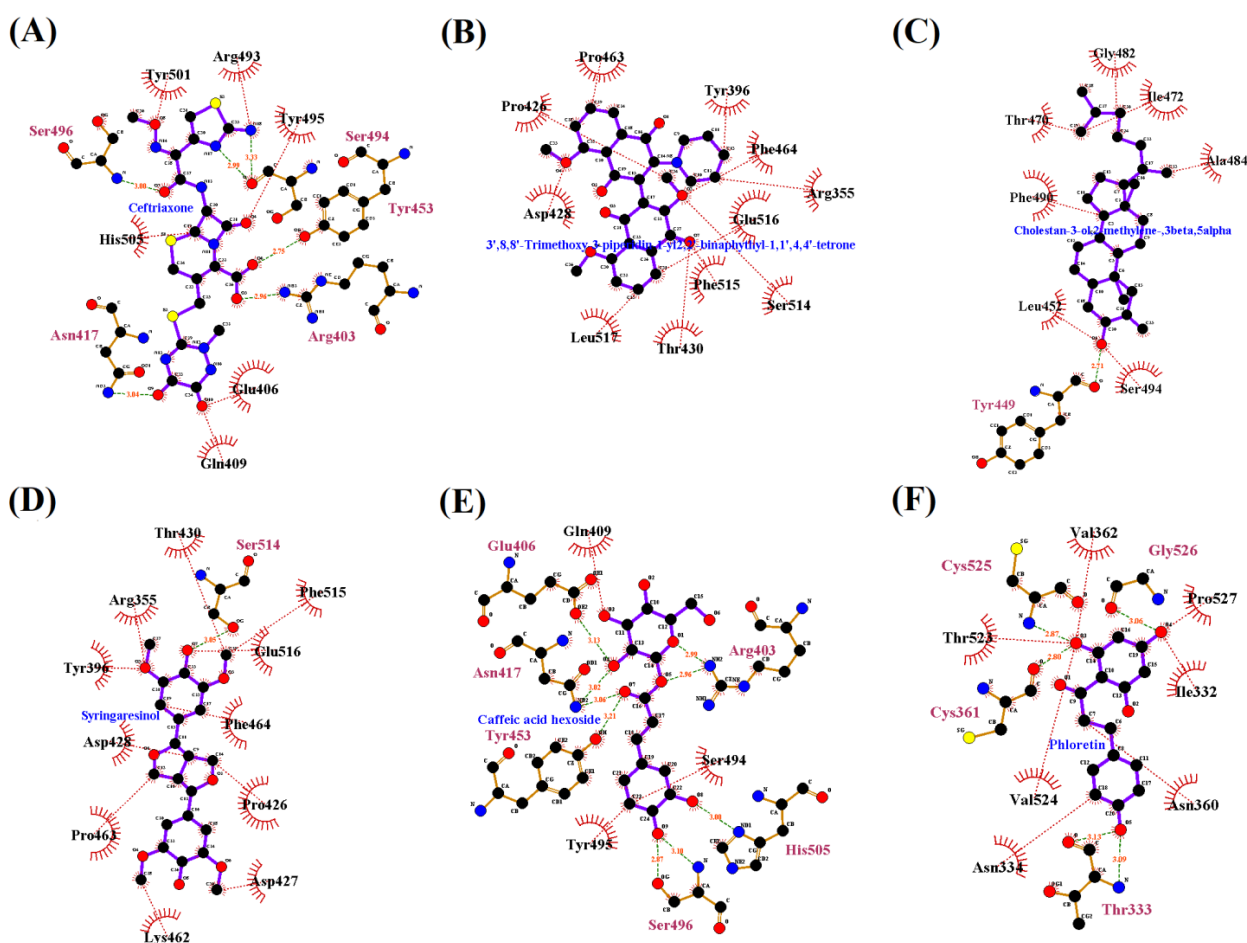


Figure 2. Cont.



**Figure 2.** The docking pose of the RBD of omicron B.1.1.529 spike protein with the most promising phytochemicals based on the binding affinity and interacting residues (A,D,G,J,M,P). The hydrophobic surface of RBD with standard drugs and seaweeds compounds (B,E,H,K,N,Q). The hydrophobicity of the interacting residues (brown (↑ hydrophobicity)-blue (↓ hydrophobicity)). The type of bonds involved in interacting phytochemicals with RBD residues (C,F,I,L,O,R).



**Figure 3.** The Ligplot interaction of the RBD of omicron B.1.1.529 spike protein with the most promising chemical compounds and standard drugs (A–F).

In addition, the Ligplot interactions between the RBD of omicron B.1.1.529 spike protein and the selected compounds such as cefuroxime, TPBT, CMBA, syringaresinol, caffeic acid hexoside, and phloretin are depicted in Figure 3.

#### 4. Discussion

Natural compounds have been utilized internationally for COVID 19 owing to their chemical variety, species diversity, and drug-like properties [48–50]. The recent experimental studies described that a lack of micro- and macronutrients in terms of quality and/or quantity in the diet of SARS-CoV-2-infected patients increases the morbidity and mortality rates [51]. Nevertheless, the intake of seaweeds as dietary supplements may provide the essential micronutrients, reducing the risk of omicron infections and organ deterioration [52,53]. The chemical compounds from the dietary seaweeds, particularly constituted with fucoidan, might have antiviral actions against SARS-CoV-2 [54]. Furthermore, seaweeds are effective against a wide spectrum of viruses such as the human immunodeficiency virus, herpes simplex, vesicular stomatitis, and cytomegalovirus [55]. Hence, in the current study, the seaweed compounds were evaluated for their antiviral activity against the binding of omicron B.1.1.529 with the ACE2 receptor.

Omicron B.1.1.529 variant had 37 mutations in the spike protein [56]. Among that, 17 mutations such as Leu371, Pro373, Phe375, Tyr396, Asp339, Lys440, Trp353, Asn417, His505, Tyr501, Arg493, Ser496, Arg498, Ser446, Ala484, Lys478, and Asn477 are reported in the RBD (Figure 1). These amino acid substitutions might have a major impact on

transmission and evasion of neutralizing mAbs, including BNT162b2, PiCoVacc, and AZD1222 vaccines [57,58].

Cefuroxime showed potential activity against protease, RNA-dependent RNA polymerase protein, and ACE2-Spike complex, which might be therapeutic ailments to fight against SARS-CoV-2 [59].

In the present study, cefuroxime exhibited a lower binding affinity ( $-5.3$  kcal/mol), and interacted with PHE375 in RBD of omicron B.1.1.529 spike protein (Figure 2A–C, Table 2). Ceftriaxone established the interaction with omicron, even though the binding affinity was  $-7.1$  kcal/mol and RMSD was  $43.189$  Å. Ceftriaxone was recommended to treat SARS-CoV-2-infected patients before ICU admission [60,61].

Bicyclo[3.2.1]oct-3-en-2-one, 3,8-dihydroxy-1-methoxy-7-(7-methoxy-1,3-benzodioxol-5-yl)-6-methyl-5 (BDBM) of *G. corticata* showed a binding affinity of  $-6.3$  kcal/mol, and RMSD of  $20.322$  Å (Table 2). Similarly, glycitein, naringenin, and pyrano [4,3-b] benzopyran-1,9-dione, 5a-methoxy-9a-methyl-3-(1-propenyl) perhydro from *P. boergeresii* showed binding affinities of  $-6.1$ ,  $-6.4$ , and  $-6.1$  kcal/mol with RMSD of  $11.668$ ,  $20.209$ , and  $29.617$  Å, respectively, to the RBD of omicron spike protein (Table 2). The increased RMSD values (thresholds  $\leq 3.0$  Å) indicated that the compounds were “unfit” to bind with the RBD of the omicron spike protein since the native structure resolution was specified as  $2.79$  Å.

Glycitein and naringenin were analyzed against the spike protein of SARS-CoV-2 and classified as antiviral flavonoids used to treat SARS-CoV-2-affected patients [62,63]. Even though the current investigation demonstrated that ceftriaxone, BDBM, glycitein, and naringenin were not really bound to the RBD of the omicron spike protein and would not be useful for the development of antiviral medications against omicron B.1.1.529, whereas cholesta-8,24-dien-3-ol, 4-methyl-, (3 beta, 4 alpha)- from *G. corticata* exhibited  $-6.8$  kcal/mol of binding affinity and  $1.544$  Å of RMSD towards the RBD, which might be useful to treat the omicron-affected patients (Table 2).

Omicron RBD mutant tightly interacts with ACE2 compared to the delta variant due to the T478K and L452R mutation [64]. Accordingly, the compound TPBT from *C. officinalis* significantly acted against the RBD of omicron spike protein, especially inhibiting the mutated residues such as TYR396 (Figure 2D–F) (Table 2). Kulkarni et al. report that the CMBA shows better binding affinity to the RBD of SARS-CoV-2 spike protein without hydrogen bonding interactions [65]. In contrast, CMBA ( $-6.0$  kcal/mol) from *C. officinalis* substantially fiddled against the RBD of omicron spike protein, especially inhibited the mutated residues L452R and E484A. Additionally, the hydrogen bond formed with the SER494 residue (Figure 2G–I) (Table 2) revealed that the CMBA compound could be strongly recommended as an antiviral drug-like compound against omicron B.1.1.529 to treat omicron-infected patients.

Adem et al. reported that caffeic acid derivatives have potential antiviral effects which also act substantially against the SARS-CoV-2 [66]. Caffeic acids have been reported for their potent virucidal activity against the herpes simplex virus, severe fever with thrombocytopenia syndrome virus, and influenza virus [67–69]. In our study, caffeic acid hexoside ( $-6.4$  kcal/mol) from *S. wightii* inhibited ASN417, SER496, TYR501, and HIS505. These residues were reported as the strongest ACE2 receptor-binding residues in the RBD of omicron spike protein (Figure 2M–O) (Table 2). The current study results distinctly demonstrated that caffeic acid hexoside had a substantial inhibitory effect against omicron B.1.1.529.

Muhammad et al. conclude that antioxidant levels are depleted due to their increased utilization in counterbalancing free radicals' negative effect. Meanwhile, the levels of erythrocytes glutathione (GSH), glutathione peroxidase (GPx), catalase, and plasma superoxide dismutase (SOD) are observed to be lower in COVID-19 patients when compared with those of controls [70]. GPx and SOD are essential antioxidant enzymes that scavenge free radicals, especially superoxide anion radicals [71]. The reduced level of GPx and SOD leads the oxidative stress and inflammation in SARS-CoV-2-affected patients [72]. Fortunately, phloretin can activate transcription factors that induce antioxidant genes' ex-

pression, improve the enzymatic antioxidant defense system, and increase SOD and GPx concentration [73]. Additionally, phloretin can be utilized as a penetration enhancer of administered drugs due to its increased fluidity towards the binding of biological membranes. Phloretin ( $-6.3$  kcal/mol) from *S. wightii* inhibited SER496, TYR501, and HIS505, which were reported as the strongest ACE2 receptor-binding residues in the RBD of omicron spike protein (Figure 2P–R) (Table 2). They suggested that the development of *S. wightii*-based dietary supplements and caffeic acid hexoside and phloretin-based antiviral medications against omicron B.1.1.529 could be feasible to manage the infection.

Glucobrassicin was reported to have inhibitory effects against SARS-CoV-2 protease [74]. Similarly, glucobrassicin from *C. racemosa* and *P. boergeri* demonstrated the significant inhibition against RBD spike protein with the binding affinity of  $-6.8$  kcal/mol, even though it did not interact with the crucial residues that bonded with the ACE2 receptor (Table 2). Glucobrassicin exhibited strong hydrogen bonding interactions with ARG457, ARG466, and ASP467 residues and may be considered for development of antiviral drugs to control the infection rate and organ damage caused by omicron B.1.1.529 (Table 2). However, additional experimental studies are needed to understand glucobrassicin's inhibitory mechanism against the omicron B.1.1.529.

A high-quality drug candidate should be effective against the therapeutic target and should also exhibit adequate ADMET qualities at therapeutic dosage to avoid drug failure in the clinical phases [75]. Hence, in this current study, we implemented a series of in silico tools to predict the ADMET properties (absorption, distribution, metabolism, excretion, and toxicity) and toxicity classes based on hepatotoxicity, carcinogenicity, immunotoxicity, mutagenicity, cytotoxicity, and the lethal dose for the resulted compounds. The classified toxicity such as hepatotoxicity, carcinogenicity, immunotoxicity, mutagenicity, and cytotoxicity might lead to liver damage, tumor formation, allergic reaction, and DNA damage. However, the functional group can be substituted by the other group of elements using the lead optimization method, which is described as a crucial part of the drug development process [76,77].

Cefuroxime possesses more than 10 hydrogen bond acceptors and exhibits mild to moderate hepatotoxicity and cytotoxicity (Table 3). Nevertheless, cefuroxime hydrophobically bonded with the crucial residue PHE375 with a reduced binding affinity (Tables 2 and 3) and showed a lesser inhibitory effect against omicron B.1.1.529.

TPBT was perfectly satisfied with drug-likeness standards ("Rule of Five" of Lipinski et al. [78]) and was found to be a more effective antiviral molecule. TPBT was bonded with TYR396 residue, which is essential for the ACE2 receptor attachment. Even though the level of toxicity was high, it was a hepatic-friendly drug that would be useful to treat omicron B.1.1.529-affected patients (Tables 2 and 3).

Similarly, the lipophilicity of the CMBA was observed as logP 8.11, which would increase the binding affinity with LEU452 and ALA484 of omicron spike protein [79,80] (Tables 2 and 3). CMBA was observed as a hepatic-friendly and a noncytotoxic candidate that would be an effective drug against omicron B.1.1.529.

Cholesta-8,24-dien-3-ol, 4-methyl-, (3 beta, 4 alpha) lipophilicity was increased, which might be the reason for the binding with TYR396 [81] (Tables 2 and 3). Like TPBT, syringaresinol also completely obeyed Lipinski's rule and bonded with the crucial residue TYR396 and was also observed as a hepatic-friendly drug with reduced cytotoxicity, which might as well be used as an antiviral drug candidate to inhibit omicron infections rate (Tables 2 and 3).

Caffeic acid hexoside contains more than five hydrogen donors and bonded with the most crucial residues of the RBD domain, such as ASN417, SER496, TYR501, and HIS505 (Tables 2 and 3). However, natural products with the violation of two or more Lipinski rules are acceptable [82]. It revealed that caffeic acid hexoside might be considered an antiviral candidate molecule, specifically against omicron B.1.1.529.

In addition, phloretin was found to be a drug-like compound [73]. Phloretin bonded with crucial residues such as SER496, TYR501, and HIS505 of RBD, which are responsible

for the binding of ACE2 receptors. Thus, phloretin would be suggested as the antiviral drug against omicron B.1.1.529 (Tables 2 and 3).

In conclusion, CMBA, caffeic acid hexoside, and phloretin are the most effective drug-like compounds against the omicron B.1.1.529 spike protein while considering the ADMET properties, drug-likeness, and the number of crucial residues such as S375F, TYR396, K417N, L452R, E484A, G496S, N501Y, and Y505H. These residues are reported as the primary cause for the strong binding of omicron B.1.1.529 with the ACE2 receptor [5]. Thus, seaweeds might be used as an important alternative dietary supplement and a promising candidate for developing antiviral drugs to treat and manage the omicron B.1.1.529 infection. However, further experiments are required to sustain the findings of the current study.

## 5. Conclusions

The present study primarily describes seaweed compounds for the inhibition of binding of RBD of omicron B.1.1.529 spike protein with the ACE2 receptor. Cholestan-3-ol, 2-methylene-, (3 beta, 5 alpha) from *C. officinalis* acted against the LEU452 and ALA484 residues of the omicron B.1.1.529 spike protein. Similarly, caffeic acid hexoside and phloretin from *S. wightii* inhibited ACE2-omicron spike protein-binding residues, specifically ASN417, SER496, TYR501, and HIS505. Further experimental studies are needed to endorse the finding of the current study. Nevertheless, our findings could help medical practitioners and dieticians to treat and manage the omicron B.1.1.529 infection. Additionally, the present study provided a strong foundation to develop antiviral drugs and/or novel food supplements from *C. officinalis* and *S. wightii*.

**Supplementary Materials:** The following supporting information can be downloaded at: <https://www.mdpi.com/article/10.3390/md20020148/s1>, Supplementary File S1: Figure S1: The Ligplot interaction between the analyzed compounds and the RBD of omicron B.1.1.529 spike protein with the binding affinity of  $\leq -6.0$  kcal/mol. (A) Ceftriaxone-RBD, (B) Cefuroxime, (C) 3',8,8'-Trimethoxy-3-piperidin-1-yl-2,2'-binaphthyl-1,1',4,4'-tetrone, (D) Cholestan-3-ol, 2-methylene-, (3beta, 5 alpha), (E) Glucobrassicin, (F) Matairesinol, (G) Naringenin, (H) Syringaresinol, (I) Bicyclo[3.2.1]oct-3-en-2-one, 3,8-dihydroxy-1-methoxy-7-(7-methoxy-1,3-benzodioxol-5-yl)-6-methyl-5, (J) Cholesta-8,24-dien-3-ol, 4-methyl-, (3.beta.,4.alpha.-), (K) Glycitein, (L) Pyrano [4,3-b] benzopyran-1,9-dione, 5a-methoxy-9a-methyl-3-(1-propenyl) perhydro, (M) 5-p-coumaroylquinic acid, (N) Caffeic acid hexoside, (O) Phloretin, (P) Querce-tin-3-O-arabinoglucoside; Table S1: The list of seaweeds and compounds utilized in the current study.

**Author Contributions:** Conceptualization, M.B., B.S.S., P.K. and C.C.; methodology, M.B. software, M.B.; validation, M.B., B.S.S. and C.C.; formal analysis, M.B.; investigation, M.B.; resources, C.C.; data curation, M.B.; writing—original draft preparation, M.B., P.K., C.C. and B.S.S.; writing—article and editing, M.B., B.S.S., P.K., S.T. and C.C.; supervision, C.C.; project administration, C.C. and B.S.S.; funding acquisition, C.C. All authors have read and agreed to the published version of the manuscript.

**Funding:** This research received funding from Chiang Mai University, Thailand.

**Institutional Review Board Statement:** Not applicable.

**Informed Consent Statement:** Not applicable.

**Data Availability Statement:** The data presented in this study are available within the article.

**Acknowledgments:** The authors gratefully acknowledge the Faculty of Pharmacy, Chiang Mai University, Chiang Mai, Thailand. This research was supported by Chiang Mai University Fund.

**Conflicts of Interest:** The authors declare no conflict of interests.

## References

1. World Health Organization. Available online: [https://www.who.int/news/item/26-11-2021-classification-of-omicron-\(b.1.1.529\)-sars-cov-2-variant-of-concern-2021](https://www.who.int/news/item/26-11-2021-classification-of-omicron-(b.1.1.529)-sars-cov-2-variant-of-concern-2021) (accessed on 19 January 2022).
2. Abdullah, F.; Myers, J.; Basu, D.; Tintinger, G.; Ueckermann, V.; Mathebula, M.; Ramlall, R.; Spoor, S.; de Villiers, T.; van der Walt, Z.; et al. Decreased severity of disease during the first global omicron variant covid-19 outbreak in a large hospital in Tshwane, South Africa. *Int. J. Infect. Dis.* **2021**, *116*, 38–42. [[CrossRef](#)] [[PubMed](#)]
3. Khare, S.; Gurry, C.; Freitas, L.; Schultz, M.B.; Bach, G.; Diallo, A.; Akite, N.; Ho, J.; Lee, R.T.; Yeo, W.; et al. GISAID's role in pandemic response. *China CDC Wkly* **2021**, *3*, 1049–1051. Available online: <https://www.gisaid.org/hcov19-variants> (accessed on 19 January 2022). [[CrossRef](#)] [[PubMed](#)]
4. Mallapaty, S. Omicron-variant border bans ignore the evidence, say scientists. *Nature* **2021**, *7888*, 199. [[CrossRef](#)] [[PubMed](#)]
5. Mannar, D.; Saville, J.W.; Zhu, X.; Srivastava, S.S.; Berezuk, A.M.; Tuttle, K.S.; Marquez, A.C.; Sekirov, I.; Subramaniam, S. SARS-CoV-2 Omicron variant: Antibody evasion and cryo-EM structure of spike protein-ACE2 complex. *Science* **2022**, eabn7760. [[CrossRef](#)]
6. Alenquer, M.; Ferreira, F.; Lousa, D.; Valério, M.; MedinaLopes, M.; Bergman, M.-L.; Goncalves, J.; Demengeot, J.; Leite, R.B.; Lilue, J.; et al. Signatures in SARS-CoV-2 spike protein conferring escape to neutralizing antibodies. *PLoS Pathog.* **2021**, *17*, e1009772. [[CrossRef](#)]
7. Dupont, L.; Snell, L.B.; Graham, C.; Seow, J.; Merrick, B.; Lechmere, T.; Maguire, T.J.A.; Hallett, S.R.; Pickering, S.; Charalampous, T.; et al. Neutralizing antibody activity in convalescent sera from infection in humans with SARS-CoV-2 and variants of concern. *Nat. Microbiol.* **2021**, *6*, 1433. [[CrossRef](#)]
8. Omotuyi, O.; Olubiyi, O.; Nash, O.; Afolabi, E.; Oyinloye, B.; Fatumo, S.; Femi-Oyewo, M.; Bogoro, S. SARS-CoV-2 Omicron spike glycoprotein receptor binding domain exhibits super-binder ability with ACE2 but not convalescent monoclonal antibody. *Comput. Biol. Med.* **2022**, *142*, 105226. [[CrossRef](#)]
9. Kazybay, B.; Ahmad, A.; Mu, C.; Mengdesh, D.; Xie, Y. Omicron N501Y mutation among SARS-CoV-2 lineages: In silico analysis of potent binding to tyrosine kinase and hypothetical repurposed medicine. *Travel Med. Infect. Dis.* **2021**, *45*, 102242. [[CrossRef](#)]
10. Ramesh, S.; Govindarajulu, M.; Parise, R.S.; Neel, L.; Shankar, T.; Patel, S.; Lowery, P.; Smith, F.; Dhanasekaran, M.; Moore, T. Emerging SARS-CoV-2 variants: A review of its mutations, its implications and vaccine efficacy. *Vaccines* **2021**, *9*, 1195. [[CrossRef](#)]
11. Zhang, L.; Cui, Z.; Li, Q.; Wang, B.; Yu, Y.; Wu, J.; Nie, J.; Ding, R.; Wang, H.; Zhang, Y.; et al. Ten emerging SARS-CoV-2 spike variants exhibit variable infectivity, animal tropism, and antibody neutralization. *Commun. Biol.* **2021**, *4*, 1196. [[CrossRef](#)]
12. Buss, L.F.; Prete, C., Jr.; Abraham, C.M.M.; Mendrone, A., Jr.; Salomon, T.; Neto, C.A.; França, R.F.O.; Belotti, M.C.; Carvalho, M.P.S.S.; Costa, A.G.; et al. Three-quarters attack rate of SARS-CoV-2 in the Brazilian Amazon during a largely unmitigated epidemic. *Science* **2021**, *371*, 288–292. [[CrossRef](#)] [[PubMed](#)]
13. Ferré, V.M.; Peiffer-Smadja, N.; Visseaux, B.; Descamps, D.; Ghosn, J.; Charpentier, C. Omicron SARS-CoV-2 variant: What we know and what we don't. *Anaesth. Crit. Care Pain Med.* **2021**, *41*, 100998. [[CrossRef](#)] [[PubMed](#)]
14. He, X.; Hong, W.; Pan, X.; Lu, G.; Wei, X. SARS-CoV-2 Omicron variant: Characteristics and prevention. *MedComm* **2021**, *2*, 838–845. [[CrossRef](#)]
15. Poudel, S.; Ishak, A.; Perez-Fernandez, J.; Garcia, E.; León-Figueroa, D.A.; Romaní, L.; Bonilla-Aldana, D.K.; Rodriguez-Morales, A.J. Highly mutated SARS-CoV-2 Omicron variant sparks significant concern among global experts—What is known so far? *Travel Med. Infect. Dis.* **2021**, *45*, 102234. [[CrossRef](#)] [[PubMed](#)]
16. Aleem, A.; Samad, A.A.B.; Slenker, A.K. *Emerging Variants of SARS-CoV-2 and Novel Therapeutics Against Coronavirus (COVID-19)*; StatPearls Publishing: Treasure Island, FL, USA, 2021.
17. Chen, J.; Wang, R.; Gilby, N.B.; Wei, G.W. Omicron variant (B.1.1.529): Infectivity, vaccine breakthrough, and antibody resistance. *J. Chem. Inf. Model* **2022**, *62*, 412–422. [[CrossRef](#)] [[PubMed](#)]
18. Awadasseid, A.; Wu, Y.; Tanaka, Y.; Zhang, W. Effective drugs used to combat SARS-CoV-2 infection and the current status of vaccines. *Biomed. Pharmacother.* **2021**, *137*, 111330. [[CrossRef](#)] [[PubMed](#)]
19. Fang, F.F.; Shi, P.Y. Omicron: A drug developer's perspective. *Emerg. Microbes Infect.* **2022**, *11*, 208–211. [[CrossRef](#)] [[PubMed](#)]
20. Rebour, C.; Marinho-Soriano, E.; Zertuche-González, J.A.; Hayashi, L.; Vásquez, J.A.; Kradolfer, P.; Soriano, G.; Ugarte, R.; Abreu, M.H.; Bay-Larsen, I.; et al. Seaweeds: An opportunity for wealth and sustainable livelihood for coastal communities. *J. Appl. Phycol.* **2014**, *26*, 1939–1951. [[CrossRef](#)]
21. Vinuganesh, A.; Kumar, A.; Prakash, S.; Alotaibi, M.O.; Saleh, A.M.; Mohammed, A.E.; Beemster, G.T.S.; AbdElgawad, H. Influence of seawater acidification on biochemical composition and oxidative status of green algae *Ulva Compressa*. *Sci. Total. Environ.* **2022**, *806*, 150445. [[CrossRef](#)]
22. Brown, E.S.; Allsopp, P.J.; Magee, P.J.; Gill, C.I.; Nitecki, S.; Strain, C.R.; McSorley, E.M. Seaweed and human health. *Nutr. Rev.* **2014**, *72*, 205–216. [[CrossRef](#)]
23. Wells, M.L.; Potin, P.; Craigie, J.S.; Raven, J.A.; Merchant, S.S.; Helliwell, K.E.; Smith, A.G.; Camire, M.E.; Brawley, S.H. Algae as nutritional and functional food sources: Revisiting our understanding. *J. Appl. Phycol.* **2017**, *29*, 949–982. [[CrossRef](#)] [[PubMed](#)]
24. Peñalver, R.; Lorenzo, J.M.; Ros, G.; Amarowicz, R.; Pateiro, M.; Nieto, G. Seaweeds as a functional ingredient for a healthy diet. *Mar. Drugs* **2020**, *18*, 301. [[CrossRef](#)] [[PubMed](#)]
25. Chen, K.K.; Minakuchi, M.; Wuputra, K.; Ku, C.C.; Pan, J.B.; Kuo, K.K.; Lin, Y.C.; Saito, S.; Lin, C.S.; Yokoyama, K.K. Redox control in the pathophysiology of influenza virus infection. *BMC Microbiol.* **2020**, *20*, 214. [[CrossRef](#)]

26. Chernyak, B.V.; Popova, E.N.; Prikhodko, A.S.; Grebenchikov, O.A.; Zinovkina, L.A.; Zinovkin, R.A. COVID-19 and oxidative stress. *Biochem.* **2020**, *85*, 1543–1553. [CrossRef] [PubMed]
27. Yang, Y.; Liu, D.; Wu, J.; Chen, Y.; Wang, S. In vitro antioxidant activities of sulfated polysaccharide fractions extracted from *Corallina officinalis*. *Int. J. Biol. Macromol.* **2011**, *49*, 1031–1037. [CrossRef] [PubMed]
28. Ismail, M.M.; Alotaibi, B.S.; El-Sheekh, M.M. Therapeutic uses of red macroalgae. *Molecules* **2020**, *25*, 4411. [CrossRef] [PubMed]
29. Yap, W.F.; Tay, V.; Tan, S.H.; Yow, Y.Y.; Chew, J. Decoding antioxidant and antibacterial potentials of Malaysian green seaweeds: *Caulerpa racemosa* and *Caulerpa Lentillifera*. *Antibiotics* **2019**, *8*, 152. [CrossRef]
30. Pangestuti, R.; Haq, M.; Rahmadi, P.; Chun, B.S. Nutritional value and biofunctionalities of two edible green seaweeds (*Ulva lactuca* and *Caulerpa racemosa*) from Indonesia by subcritical water hydrolysis. *Mar. Drugs* **2021**, *19*, 578. [CrossRef]
31. Lorente, L.; Martín, M.M.; González-Rivero, A.F.; Pérez-Cejas, A.; Argueso, M.; Perez, A.; Ramos-Gómez, L.; Solé-Violán, J.; Marcos, Y.; Ramos, J.A.; et al. Blood concentrations of proapoptotic sFas and antiapoptotic Bcl2 and COVID-19 patient mortality. *Expert Rev. Mol. Diagn.* **2021**, *21*, 837–844. [CrossRef]
32. Monla, A.R.; Dassouki, Z.; Kouzayha, A.; Salma, Y.; Gali-Muhtasib, H.; Mawlawi, H. The cytotoxic and apoptotic effects of the brown algae *Colpomenia sinuosa* are mediated by the generation of reactive oxygen species. *Molecules* **2020**, *25*, 1993. [CrossRef]
33. Rosemary, T.; Arulkumar, A.; Paramasivam, S.; Mondragon-Portocarrero, A.; Miranda, J.M. Biochemical, micronutrient and physicochemical properties of the dried red seaweeds *Gracilaria edulis* and *Gracilaria Corticata*. *Molecules* **2019**, *24*, 2225. [CrossRef] [PubMed]
34. Asghar, A.; Tan, Y.C.; Shahid, M.; Yow, Y.Y.; Lahiri, C. Metabolite profiling of malaysian *Gracilaria edulis* reveals eplerenone as novel antibacterial compound for drug repurposing against MDR bacteria. *Front. Microbiol.* **2021**, *12*, 653562. [CrossRef]
35. Ali, L.; Khan, A.L.; Al-Broumi, M.; Al-Harrasi, R.; Al-Kharusi, L.; Hussain, J.; Al-Harrasi, A. New enzyme-inhibitory triterpenoid from marine macro brown alga *Padina boergesenii* allender & kraft. *Mar. Drugs* **2017**, *15*, 19.
36. Gora, A.H.; Sahu, N.P.; Sahoo, S.; Rehman, S.; Ahmad Dar, S.; Ahmad, I.; Agarwal, D. Effect of dietary *Sargassum wightii* and its fucoidan-rich extract on growth, immunity, disease resistance and antimicrobial peptide gene expression in *Labeo rohita*. *Int. Aquat. Res.* **2018**, *10*, 115–131. [CrossRef]
37. Kumar, Y.; Tarafdar, A.; Kumar, D.; Badgujar, P.C. Effect of indian brown seaweed *Sargassum wightii* as a functional ingredient on the phytochemical content and antioxidant activity of coffee beverage. *J. Food Sci. Technol.* **2019**, *56*, 4516–4525. [CrossRef] [PubMed]
38. Eberhardt, J.; Santos-Martins, D.; Tillack, A.F.; Forli, S. AutoDock vina 1.2.0: New docking methods, expanded force field, and python bindings. *J. Chem. Inf. Model.* **2021**, *61*, 3891–3898. [CrossRef] [PubMed]
39. Dallakyan, S.; Olson, A.J. Small-molecule library screening by docking with PyRx. *Methods Mol. Biol.* **2015**, *1263*, 243–250.
40. Lill, M.A.; Danielson, M.L. Computer-aided drug design platform using PyMOL. *J. Comput. Aided Mol. Des.* **2011**, *25*, 13–19. [CrossRef]
41. Laskowski, R.A.; Swindells, M.B. LigPlot+: Multiple ligand-protein interaction diagrams for drug discovery. *J. Chem. Inf. Model.* **2011**, *51*, 2778–2786. [CrossRef]
42. Grob, S. Slovakia. Molinspiration Cheminformatics Free Web Services. Available online: <https://www.molinspiration.com> (accessed on 15 January 2022).
43. Xiong, G.; Wu, Z.; Yi, J.; Fu, L.; Yang, Z.; Hsieh, C.; Yin, M.; Zeng, X.; Wu, C.; Lu, A.; et al. ADMETlab 2.0: An integrated online platform for accurate and comprehensive predictions of ADMET properties. *Nucleic Acids Res.* **2021**, *49*, W5–W14. [CrossRef]
44. Banerjee, P.; Eckert, A.O.; Schrey, A.K.; Preissner, R. ProTox-II: A webserver for the prediction of toxicity of chemicals. *Nucleic Acids Res.* **2018**, *46*, W257–W263. [CrossRef] [PubMed]
45. Burley, S.K.; Berman, H.M.; Kleywegt, G.J.; Markley, J.L.; Nakamura, H.; Velankar, S. Protein Data Bank (PDB): The single global macromolecular structure archive. *Methods Mol. Biol.* **2017**, *1607*, 627–641. [PubMed]
46. Kim, S.; Chen, J.; Cheng, T.; Gindulyte, A.; He, J.; He, S.; Li, Q.; Shoemaker, B.A.; Thiessen, P.A.; Yu, B.; et al. PubChem in 2021: New data content and improved web interfaces. *Nucleic Acids Res.* **2021**, *49*, D1388–D1395. [CrossRef]
47. O’Boyle, N.M.; Banck, M.; James, C.A.; Morley, C.; Vandermeersch, T.; Hutchison, G.R. Open Babel: An open chemical toolbox. *J. Cheminform.* **2011**, *73*, 33. [CrossRef] [PubMed]
48. Mani, J.S.; Johnson, J.B.; Steel, J.C.; Broszczak, D.A.; Neilsen, P.M.; Walsh, K.B.; Naiker, M. Natural product-derived phytochemicals as potential agents against coronaviruses: A review. *Virus Res.* **2020**, *284*, 197989. [CrossRef] [PubMed]
49. Teli, D.M.; Shah, M.B.; Chhabria, M.T. In silico screening of natural compounds as potential inhibitors of SARS-CoV-2 main protease and spike RBD: Targets for COVID-19. *Front. Mol. Biosci.* **2021**, *7*, 599079. [CrossRef]
50. Bharathi, M.; Sivamaruthi, B.S.; Kesika, P.; Thangaleela, S.; Chaiyasut, C. In silico screening of potential phytocompounds from several herbs against sars-cov-2 indian delta variant b.1.617.2 to inhibit the spike glycoprotein trimer. *Appl. Sci.* **2022**, *12*, 665. [CrossRef]
51. Jayawardena, R.; Sooriyaarachchi, P.; Chourdakis, M.; Jeewandara, C.; Ranasinghe, P. Enhancing immunity in viral infections, with special emphasis on COVID-19: A review. *Diabetes Metab. Syndr.* **2020**, *14*, 367–382. [CrossRef]
52. Leandro, A.; Pacheco, D.; Cotas, J.; Marques, J.C.; Pereira, L.; Gonçalves, A.M.M. Seaweed’s bioactive candidate compounds to food industry and global food security. *Life* **2020**, *10*, 140. [CrossRef]
53. Ahmed, M.H.; Hassan, A.; Molnár, J. The role of micronutrients to support immunity for covid-19 prevention. *Rev. Bras. Farmacogn.* **2021**, *31*, 361–374. [CrossRef]

54. Tamama, K. Potential benefits of dietary seaweeds as protection against COVID-19. *Nutr. Rev.* **2021**, *79*, 814–823. [[CrossRef](#)] [[PubMed](#)]
55. Bai, R.G.; Tuvikene, R. Potential antiviral properties of industrially important marine algal polysaccharides and their significance in fighting a future viral pandemic. *Viruses* **2021**, *13*, 1817.
56. McMahan, K.; Yu, J.; Mercado, N.B.; Loos, C.; Tostanoski, L.H.; Chandrashekar, A.; Liu, J.; Peter, L.; Atyeo, C.; Zhu, A.; et al. Correlates of protection against SARS-CoV-2 in rhesus macaques. *Nature* **2021**, *590*, 630–634. [[CrossRef](#)]
57. Collie, S.; Champion, J.; Moultrie, H.; Bekker, L.G.; Gray, G. Effectiveness of BNT162b2 vaccine against omicron variant in South Africa. *N. Engl. J. Med.* **2022**, *386*, 494–496. [[CrossRef](#)] [[PubMed](#)]
58. Peiris, M.; Cheng, S.; Mok, C.K.P.; Leung, Y.; Ng, S.; Chan, K.; Ko, F.; Yiu, K.; Lam, B.; Lau, E.; et al. Neutralizing antibody titres to SARS-CoV-2 Omicron variant and wild-type virus in those with past infection or vaccinated or boosted with mRNA BNT162b2 or inactivated CoronaVac vaccines. *Res. Sq.* **2022**, rs.3.rs-1207071, Preprint. [[CrossRef](#)]
59. Durojaiye, A.B.; Clarke, J.D.; Stamatiades, G.A.; Wang, C. Repurposing cefuroxime for treatment of COVID-19: A scoping review of in silico studies. *J. Biomol. Struct. Dyn.* **2021**, *39*, 4547–4554. [[CrossRef](#)]
60. Adebisi, Y.A.; Jimoh, N.D.; Ogunkola, I.O.; Uwizeyimana, T.; Olayemi, A.H.; Ukor, N.A.; Lucero-Prisno, D.E., 3rd. The use of antibiotics in COVID-19 management: A rapid review of national treatment guidelines in 10 African countries. *Trop. Med. Health.* **2021**, *49*, 51. [[CrossRef](#)]
61. Mustafa, L.; Tolaj, I.; Baftiu, N.; Fejza, H. Use of antibiotics in COVID-19 ICU patients. *J. Infect. Dev. Ctries.* **2021**, *15*, 501–505. [[CrossRef](#)]
62. Alberca, R.W.; Teixeira, F.M.E.; Beserra, D.R.; de Oliveira, E.A.; Andrade, M.M.S.; Pietrobon, A.J.; Sato, M.N. Perspective: The potential effects of naringenin in COVID-19. *Front. Immunol.* **2020**, *11*, 570919. [[CrossRef](#)]
63. Shawan, M.M.A.K.; Halder, S.K.; Hasan, M.A. Luteolin and abyssinone II as potential inhibitors of SARS-CoV-2: An in silico molecular modeling approach in battling the COVID-19 outbreak. *Bull. Natl. Res. Cent.* **2021**, *45*, 27. [[CrossRef](#)]
64. Wu, L.; Zhou, L.; Mo, M.; Liu, T.; Wu, C.; Gong, C.; Lu, K.; Gong, L.; Zhu, W.; Xu, Z. The effect of the multiple mutations in Omicron RBD on its binding to human ACE2 receptor and immune evasion: An investigation of molecular dynamics simulations. *ChemRxiv. Camb. Camb. Open Engag.* **2021**. Preprint. [[CrossRef](#)]
65. Kulkarni, S.A.; Krishnan, S.B.B.; Chandrasekhar, B.; Banerjee, K.; Sohn, H.; Madhavan, T. Characterization of phytochemicals in *Ulva intestinalis* L. and their action against SARS-CoV-2 spike glycoprotein receptor-binding domain. *Front. Chem.* **2021**, *27*, 735768. [[CrossRef](#)] [[PubMed](#)]
66. Adem, Ş.; Eyupoglu, V.; Sarfraz, I.; Rasul, A.; Zahoor, A.F.; Ali, M.; Abdalla, M.; Ibrahim, I.M.; Elfiky, A.A. Caffeic acid derivatives (CAFDs) as inhibitors of SARS-CoV-2: CAFDs-based functional foods as a potential alternative approach to combat COVID-19. *Phytomedicine* **2021**, *85*, 153310. [[CrossRef](#)] [[PubMed](#)]
67. Utsunomiya, H.; Ichinose, M.; Ikeda, K.; Uozaki, M.; Morishita, J.; Kuwahara, T.; Koyama, A.H.; Yamasaki, H. Inhibition by caffeic acid of the influenza A virus multiplication in vitro. *Int. J. Mol. Med.* **2014**, *34*, 1020–1024. [[CrossRef](#)]
68. Ogawa, M.; Shirasago, Y.; Ando, S.; Shimojima, M.; Saijo, M.; Fukasawa, M. Caffeic acid, a coffee-related organic acid, inhibits infection by severe fever with thrombocytopenia syndrome virus in vitro. *J. Infect. Chemother. Off. J. Jpn. Soc. Chemother.* **2018**, *24*, 597–601. [[CrossRef](#)] [[PubMed](#)]
69. Langland, J.; Jacobs, B.; Wagner, C.E.; Ruiz, G.; Cahill, T.M. Antiviral activity of metal chelates of caffeic acid and similar compounds towards herpes simplex, VSV-Ebola pseudotyped and vaccinia viruses. *Antivir. Res.* **2018**, *160*, 143–150. [[CrossRef](#)]
70. Muhammad, Y.; Kani, Y.A.; Iliya, S.; Muhammad, J.B.; Binji, A.; Ahmad, E.A.; Kabir, M.B.; Bindawa, U.K.; Ahmed, A. Deficiency of antioxidants and increased oxidative stress in COVID-19 patients: A cross-sectional comparative study in Jigawa, Northwestern Nigeria. *SAGE Open Med.* **2021**, *9*, 2050312121991246. [[CrossRef](#)] [[PubMed](#)]
71. Ighodaro, O.M.; Akinloye, O.A. First line defence antioxidants-superoxide dismutase (SOD), catalase (CAT) and glutathione peroxidase (GPX): Their fundamental role in the entire antioxidant defence grid. *Alex. J. Med.* **2018**, *54*, 287–293. [[CrossRef](#)]
72. Beltrán-García, J.; Osca-Verdegal, R.; Pallardó, F.V.; Ferreres, J.; Rodríguez, M.; Mulet, S.; Sanchis-Gomar, F.; Carbonell, N.; García-Giménez, J.L. Oxidative stress and inflammation in COVID-19-associated sepsis: The potential role of anti-oxidant therapy in avoiding disease progression. *Antioxidants* **2020**, *9*, 936. [[CrossRef](#)]
73. Behzad, S.; Sureda, A.; Barreca, D.; Nabavi, S.F.; Rastrelli, L.; Nabavi, S.M. Health effects of phloretin: From chemistry to medicine. *Phytochem. Rev.* **2017**, *16*, 527–533. [[CrossRef](#)]
74. Fadaka, A.O.; Sibuyi, N.R.S.; Martin, D.R.; Klein, A.; Madiehe, A.; Meyer, M. Development of effective therapeutic molecule from natural sources against coronavirus protease. *Int. J. Mol. Sci.* **2021**, *22*, 9431. [[CrossRef](#)]
75. Guan, L.; Yang, H.; Cai, Y.; Sun, L.; Di, P.; Li, W.; Liu, G.; Tang, Y. ADMET-score—A comprehensive scoring function for evaluation of chemical drug-likeness. *Medchemcomm* **2018**, *10*, 148–157. [[CrossRef](#)] [[PubMed](#)]
76. Benkerroum, N. Chronic and acute toxicities of aflatoxins: Mechanisms of action. *Int. J. Environ. Res. Public Health.* **2020**, *17*, 423. [[CrossRef](#)] [[PubMed](#)]
77. Wang, S.; Dong, G.; Sheng, C. Structural simplification: An efficient strategy in lead optimization. *Acta. Pharm. Sin. B.* **2019**, *9*, 880–901. [[CrossRef](#)] [[PubMed](#)]
78. Lipinski, C.A.; Lombardo, F.; Dominy, B.W.; Feeney, P.J. Experimental and computational approaches to estimate solubility and permeability in drug discovery and development settings. *Adv. Drug Deliv. Rev.* **2012**, *64*, 4–17. [[CrossRef](#)]

79. Jayaraj, V.; Suhanya, R.; Vijayasathy, M.; Anandagopu, P.; Rajasekaran, E. Role of large hydrophobic residues in proteins. *Bioinformatics* **2009**, *3*, 409–412. [[CrossRef](#)]
80. Weinstein, J.Y.; Elazar, A.; Fleishman, S.J. A lipophilicity-based energy function for membrane-protein modelling and design. *PLoS Comput. Biol.* **2019**, *15*, e1007318. [[CrossRef](#)]
81. Gowder, M.S.; Chatterjee, J.; Chaudhuri, T.; Paul, K. Prediction and analysis of surface hydrophobic residues in tertiary structure of proteins. *Sci. World J.* **2014**, *2014*, 971258.
82. Benet, L.Z.; Hosey, C.M.; Ursu, O.; Oprea, T.I. BDDCS, the Rule of 5 and drugability. *Adv. Drug. Deliv. Rev.* **2016**, *101*, 89–98. [[CrossRef](#)]